Time-domain measurements of Rydberg doublet splittings using microwave half-cycle pulses

C. W. S. Conover and M. C. Doogue*
Physics Department, Colby College, Waterville, Maine 04901
(Received 14 July 2000; published 7 February 2001)

We observe transitions between Rydberg states driven by intense 500-ps-wide half-cycle electric-field pulses in a microwave transmission line. Using two identical temporally spaced pulses we can perform spectroscopic measurements. We have measured fine-structure intervals between the $d_{3/2}$ and $d_{5/2}$ states in Na and K using this technique. The frequency measurements span two orders of magnitude and are an order of magnitude more accurate than previous direct measurements of these transitions and more than a factor of 2 more accurate than previous high-precision microwave measurements.

DOI: 10.1103/PhysRevA.63.032504 PACS number(s): 32.10.Dk, 32.80.Wr, 32.30.Bv

I. INTRODUCTION

We have developed a time-domain technique for accurately measuring frequency intervals between Rydberg states of atoms and molecules. Using intense half-cycle microwave pulses (HCP's), transitions can be driven between different Rydberg states. By delaying two HCP's, a Ramsey interference measurement of frequency intervals can be performed. This HCP-Ramsey technique is applicable to the measurement of both large and small frequency intervals, both for allowed and forbidden transitions. In this article we describe the technique and present measurements of the fine-structure intervals of sodium and potassium nd Rydberg states. We have measured fine-structure intervals for principal quantum numbers ranging from 15 to 30, with frequencies ranging from 2.5 to 250 MHz.

The structure and dynamics of Rydberg atoms continue to be of significant interest both because of the close connection of their wavefunctions to those of hydrogen and the rich variety of behavior that they show [1]. In Rydberg states, the fine-structure intervals can be anomalously large and even inverted despite the nearly hydrogenic term energies. In particular, the calculation of fine-structure intervals at the boundary between core penetrating and nonpenetrating orbits in Rydberg atoms has proven to be a challenge for theory. In the nd series relativistic effects, along with both penetration and polarization energy shifts, are significant and the fine structure is known to be inverted in both sodium and potassium. The precise measurement of these intervals provides a stringent test of theoretical models [2–4].

In the HCP-Ramsey method, a strong microwave HCP drives transitions between Rydberg states, leaving a coherent superposition of states, each of which evolves at its natural frequency. A second, delayed, HCP again redistributes population, with the final population of each state depending on the phases accumulated by the different states in the field-free time interval between the two pulses. The atoms are then exposed to a selective field ionization pulse and the population in each state can be observed as a function of delay between the HCP's. A discrete Fourier transform of the ionization signal gives the energy differences. In the HCP-Ramsey method the amplitude of the periodic signal can be nearly 100% of the total ionization signal for correctly chosen HCP voltages. Because the population is transferred by strong field interactions, the maximum measured frequency interval is not limited by the bandwidth of the HCP, but only by the homogeneity of the HCP field and by the relative phase jitter between the two HCPs. Further, in the strong-field regime, the population of a single bound state contains information about all bound levels populated during the HCP, which means that measurement of the population of a single state allows determination of the frequency differences between all of the states that are populated by the HCP's [5]. The HCP method is applicable to significantly higher frequencies than presented here, and we have measured frequency intervals greater than 70 GHz between ns and nd states with HCPs of approximately 1 GHz bandwidth [6].

In the case of the fine structure measurements, the transitions are essentially Rosen–Zener type of noncrossing transitions [7,8]. These transitions are strong if the HCP pulse is short compared to the inverse of the frequency separation of the two levels and if the relative phase accumulated by the two states during the HCP is $n\pi$. In both sodium and potassium the 500 ps half-cycle pulses easily satisfy the first criterion, and in sodium they are strong enough to give 100% population transfer. In potassium, however, because the polarizabilities are so much smaller, the relative phase accumulated during the pulse is such that we cannot achieve 100% population transfer with the current setup.

II. EXPERIMENT

We observe the microwave HCP driven transitions in an atomic beam. The main features of the apparatus have been described earlier [6]. A thermal beam of atoms passes between the parallel plates of a 50 Ω transmission line, shown schematically in Fig. 1. The atoms are excited in a stepwise manner to selected nd Rydberg states by two pulsed dye lasers. Particular n, j, and $|m_j|$ states can be selected by changing the colors and polarizations of the dye lasers.

About 100 ns after the Rydberg states are populated, a pair of relatively delayed 500 ps FWHM HCP's with amplitudes up to 100 V/cm, produced by a pair of Avtech AVH-HV1 impulse generators, are incident on the Rydberg atoms.

*Currently at the Allegro MicroSystems, Concord, NH.

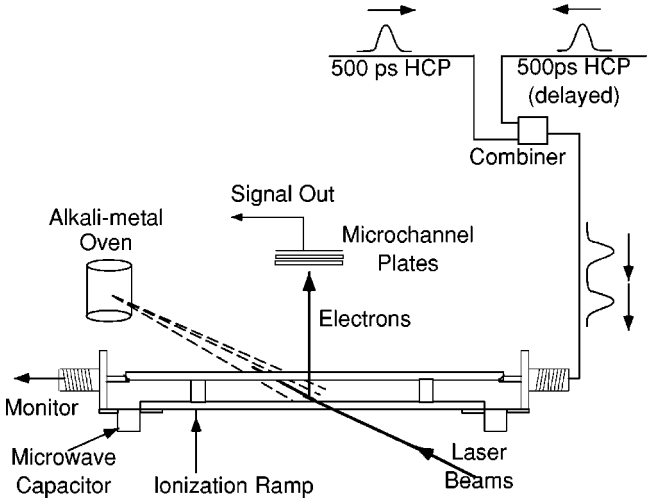

FIG. 1. Diagram of the main features of the experimental apparatus showing the pulse delay scheme, parallel plate transmission line, atomic source, and microchannel plate detectors. The atomic and laser beams are antiparallel with the laser polarization in the vertical direction. The transmission line is constructed of brass with SMA connectors and 100 pF microwave capacitors used to couple the HCP onto the line while isolating the bottom plate from ground to allow a state-selective field ionization pulse to be applied. A 0.5 mm hole drilled in the top plate of the transmission line allows electrons from the ionized atoms to reach the detector.

We have measured the pulse shape in the interaction region with a 1.5 GHz bandwidth oscilloscope and a high-bandwidth 500 Ω probe. The pulse shape is approximated by the form

$$F(t)=F_0 \sin^4\left(\pi \frac{t}{\tau}\right), \tag{1}$$

where τ is the full-width of the field pulse and F_0 is the peak amplitude. For numerical models of the interaction of the atoms with a half-cycle pulse we used the form of Eq. (1) with $\tau=1.30$ ns to match the width of the pulse measured in the laboratory.

The population redistributed by a single HCP remains coherent at the end of the first pulse, and there is a well-defined phase difference between the fine-structure states after the pulse. When the second HCP is incident on the atoms, population is again redistributed, and the final population in each state depends both on the shape and amplitude of the two pulses and, most significantly for these experiments, the relative phase accumulated by the two states in the field-free period between the two pulses. There is a small, long (10–20 ns) negative tail on the HCP which is avoided by using a minimum delay between the HCP's of 50 ns.

Then, 100 ns after the second HCP, a large electric field ramp is applied to one side of the transmission line. As seen in Fig. 1, microwave capacitors isolate the lower plate from ground and allow the application of this high voltage. This high-voltage ramp both ionizes the Rydberg atoms and pushes the electrons through a small hole in the top plate of the transmission line toward a microchannel plate detector. Rydberg states ionize at a characteristic field and therefore at different times during a voltage ramp, so the time of arrival of the electrons at a detector can be used to distinguish the number of atoms in a particular state. In particular, states of different j, but the same ℓ and m_j, can be distinguished by field ionization [9]. In order to measure the population in the two fine-structure states, the signal from the detector is sent to two boxcar integrators which are gated to measure electrons from each of the two fine-structure states. The output of the integrator is sent to an analog-to-digital converter and read by the computer which also controls the HCP amplitudes and relative delays.

In Na we excite the $d_{3/2}$ $m_j=1/2$ state and drive transitions to the $d_{5/2}$ $m_j=1/2$ with the HCP's. When the ionizing field is slowly turned on, the $d_{3/2}$ $m_j=1/2$ state adiabatically evolves into the $m_\ell=1$ state, and the $d_{5/2}$ $m_j=1/2$ state adiabatically turns into the $m_\ell=0$ state [10]. The $m_\ell=0$ state ionizes at a lower field than the $m_\ell=1$ state, making it easy to use selective ramped field ionization to measure the populations in each of the m_j states. In K the situation is not so simple and the ionization thresholds of the doublet $m_j=1/2$ states are not distinguishable [11] and it is impossible to perform the experiment with the $m_j=1/2$ states. However, it has been shown that part of the population of the $d_{3/2}$ $m_j=3/2$ state ionizes at a higher level than the $d_{5/2}$ $m_j=3/2$ state, and can be used to selectively detect a $\Delta m_j=0$ transition between the fine structure levels [12]. The benefit of using the $|m_j|=1/2$ states is that they are an order of magnitude less susceptible to stray electric fields than the $|m_j|=3/2$ states.

Both lasers are antiparallel to the atomic beam, exciting a cylindrical volume of atoms about 1 mm in diameter, which allows a wide variety of time delays without realignment of the optics. The atomic beam crosses the transmission line transverse to the direction of HCP travel, limiting the effect of delay changes due to atomic motion: the time domain equivalent of Doppler broadening. The maximum delay time is limited to the transit time of the atoms across the 2 cm interaction region. The delays are swept electronically and several delay sweeps are made for each measurement to reduce the effect of long-term drifts in the atomic beam or laser intensities.

There are several systematic effects which must be considered in Rydberg atom spectroscopy. The measured frequencies can be systematically shifted by two important effects, AC and DC Stark shifts. In addition, the spectral lines are broadened by several effects, radiative decay lifetimes, interactions with blackbody radiation, phase noise in the HCP delay, fluctuations in the HCP amplitude, the Zeeman effect, and collisions.

In the experiments presented here, the width of the spectral lines measured is mainly due to the atoms' decay rate. The decay of the states is due to a combination of the natural lifetime and transitions induced by 300 K blackbody radiation. For the states we have studied, the total decay rates range from 2.5 to 15 μs [1]. Collisional broadening due to background gas is calculated to be negligible in our vacuum, however collisions between Rydberg atoms may be significant at the largest principal quantum numbers. Zeeman

broadening is reduced by firing the lasers synchronously with the zero crossings of the line voltage. In addition, the transmission line is surrounded by an open ended rectangular box constructed of mu-metal, and the interaction region is also placed at the center of a pair of vertically oriented Helmholtz coils that eliminate the majority of the earth's magnetic field in the interaction region. These precautions reduce the magnetic field in the interaction region to less than 0.1 G. The Zeeman beat period is approximately 10 μs, on the order of the transit time.

Particular to the HCP-Ramsey technique, there are two important sources of broadening: delay jitter and amplitude inhomogeneity. If there is variation in the HCP amplitude, the dynamical phase accumulated during the HCP will be different for different atoms, which broadens the spectral line. Experiments with *s* state to high-ℓ state transitions in sodium, where the relative Stark shifts of 500–1000 MHz/(V/cm) due to the linear Stark effect for the high-ℓ states are much larger than in these experiments, show that the amplitude jitter and inhomogeneity are unimportant effects. Shot-to-shot jitter in the relative pulse delay is the largest experimentally controllable source of broadening. The two impulse generators are triggered with a computer controlled Stanford Research Systems SR535 digital delay generator with a temperature compensated crystal oscillator. The SR535 has a rms jitter of 50 ps for the delays used in these experiments. Additionally the AVH-HV1 also has a 15 ps jitter in the delay between a trigger signal and the output HCP. The jitter in the HCP delay is a broadening mechanism, and for the data presented here it adds 15 kHz to the linewidth at the highest frequencies measured, but becomes much more important for larger frequency intervals. The timing jitter in the HCP delays limits the upper frequency range of the current apparatus to less than 5 GHz. In the results presented here, these instrumental imperfections add an unmeasurable amount of broadening.

By far the most important systematic concern in Rydberg spectroscopy is Stark shifts. Normally, when using strong fields to drive forbidden transitions, care must be taken regarding AC Stark shifts of the levels due to the driving field. However, the phase differences measured in the HCP-Ramsey method depend only on the energy levels in the field-free interval between the two pulses, and the large Stark shifts that exist during the HCP's are unimportant. AC Stark shifts of Rydberg states due to the interaction with blackbody radiation can be comparable to the fine-structure intervals measured. However, these shifts affect both states in the doublet equally and are therefore not measured [1].

For our experiments, the largest systematic effect is DC Stark shifts due to stray electric fields. In a small static electric field the energy levels shift by an amount

$$\Delta E_{n\ell j m_j} = -\frac{1}{2}\left[\alpha^S_{n\ell} + \alpha^T_{n\ell j}\left(\frac{3m_j^2 - j(j+1)}{j(2j-1)}\right)\right]F^2, \quad (2)$$

where α^S is the scalar polarizability and α^T is the tensor polarizability [13,14]. The scalar polarizability is the same for all levels in the given $n\ell$ shell, and characterizes a shift in the center of gravity of the multiplet. The tensor polarizability depends on *j*, and characterizes the differential Stark shift within the multiplet. The tensor polarizability for a given multiplet, $\alpha^T_{n\ell}$, is defined as the polarizability of the state with maximum *j* within the multiplet. For a Rydberg doublet, the splittings in a small static field are

$$\Delta_{m_j}(F) = \Delta_0 + \alpha^T_{nl}F^2\left\{\frac{6m_j^2}{(2\ell-1)\ell(2\ell+1)}\right\} \quad (3)$$

and for the doublets of the d states

$$\Delta_{1/2}(F) = \Delta_o + \frac{\alpha^T_{nd}}{20}F^2, \quad (4)$$

$$\Delta_{3/2}(F) = \Delta_o + \frac{9\alpha^T_{nd}}{20}F^2, \quad (5)$$

where Δ_o is the field-free fine-structure interval. The fine-structure intervals for the $m_j = 1/2$ transitions are nine times less susceptible to stray fields than the $m_j = 3/2$ transitions and therefore are much more appropriate for the experiments.

The polarizabilities depend on the matrix elements of the electric dipole operator, which are readily calculated numerically. The polarizabilities increase rapidly with ℓ and effective quantum number, in alkali atoms scaling as n^{*7}. We have calculated the polarizabilities and estimate the tensor polarizability in sodium to be given by the equation $\alpha^T_{nd}(\mathrm{Na}) = 5.2\times10^{-9}n^{*7}$ MHz$(\mathrm{V/cm})^{-2}$, while in potassium $\alpha^T_{nd}(\mathrm{K}) = 1.1\times10^{-10}n^{*7}$ MHz$(\mathrm{V/cm})^{-2}$, 50 times smaller than the polarizabilities in Na.

Standard precautions [15] reduced the stray field in the interaction region to less than 35 mV/cm. We periodically determined the stray field by measuring the fine structure splitting with known offset fields and finding the field required to minimize the fine structure interval. Empirically, these stray fields change day to day, probably in large part due to alkali deposition on the plates. Using the calculated tensor polarizabilities, we have added the fourth column to our data tables, showing how a stray field of 70 mV/cm in the transmission line affects the measured fine-structure intervals. It is clear that at low principal quantum number, the DC Stark effect has essentially no influence on the data, but at higher principal quantum number it becomes the dominant source of error.

III. RESULTS

For properly chosen HCP amplitudes significant population is transferred between the fine-structure levels, but very little population is transferred to the high-ℓ states. An example of the population transfer due to a single HCP is shown in Fig. 2, which shows the population of the $23d_{3/2}$ and $23d_{5/2}$ states in sodium as a function of peak HCP field. At higher amplitudes some population is transferred to high-ℓ states, and that population is not detected in our selective detection scheme. Previous experiments have detected and analyzed the transitions to high-ℓ states [6].

The solid lines in Fig. 2 were calculated by numerically

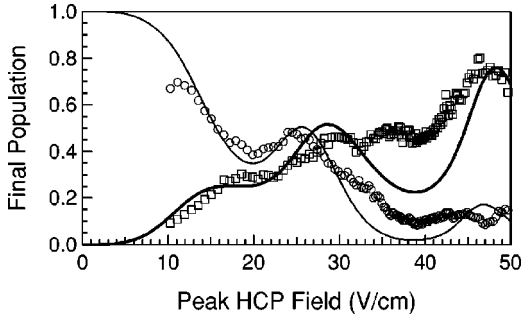

FIG. 2. Plot of population in the $23d_{3/2}$ (○) and $23d_{5/2}$ (□) states versus peak amplitude after a single HCP. The solid lines were calculated numerically with Schrödinger's equation on a limited basis.

integrating the time-dependent Schrödinger equation using a finite basis and the model of the pulse given by Eq. (1). Population transfer depends strongly on the relative phase accumulated by all states with $\ell \geq 2$ during the pulse. Differences between the calculated and observed transfer probabilities is attributed to an imperfect knowledge of the pulse shape.

The results of single pulse experiments with variable amplitude are similar for those with potassium, but the fields required are significantly larger, due to their much smaller polarizabilities. No population is transferred out of the d states because of their isolation from other states. Finally, it is difficult, due to the properties of field ionization in potassium, to unambiguously identify the population in the $d_{3/2}$ and $d_{5/2}$ states.

We have measured population as a function of relative HCP delay for a variety of principal quantum numbers in the range from 15 to 30. Typical traces of the $d_{3/2}$ and $d_{5/2}$ population versus relative pulse delay is shown in Fig. 3. Figure 3(a) shows the populations of the sodium $23d_{3/2}$ and $23d_{5/2}$ states. The magnitude of the two HCP's was 20 V/cm and the absolute pulse delay is unknown to 5 ns. The ratio of the oscillating component to the total ionization signal is roughly 70%. This contrast ratio is reduced if the two HCP's are not identical and if there is significant population of the high-ℓ states by the HCP's. Notice that in Fig. 3(a) the total d state population is not a constant, and that population transfer to high-ℓ states also depends on the relative phases of the coherent superposition as well as the amplitudes of the pulses.

Figure 3(b) shows data for 80 V/cm HCP's applied to potassium 19d states. The modulation depth is much smaller in the potassium data. First, with the HCP's we used, the relative phase accumulated during the pulse is much less than π, and we cannot saturate the transition between the fine structure levels. Second, the field ionization of the $d_{3/2}$ and $d_{5/2}$ levels is not clearly resolved.

Data such as those shown in Fig. 3 have been taken for time delays of up to 20 μs. Discrete Fourier transforms of typical data are shown in Fig. 4 , along with Lorentzian fits to the data. The spectral lines are quite well approximated by Lorentzian lineshapes with widths of 150–300 kHz. Many measurements of spectra like those in Fig. 4 have been taken over the course of several months, and the statistical uncer-

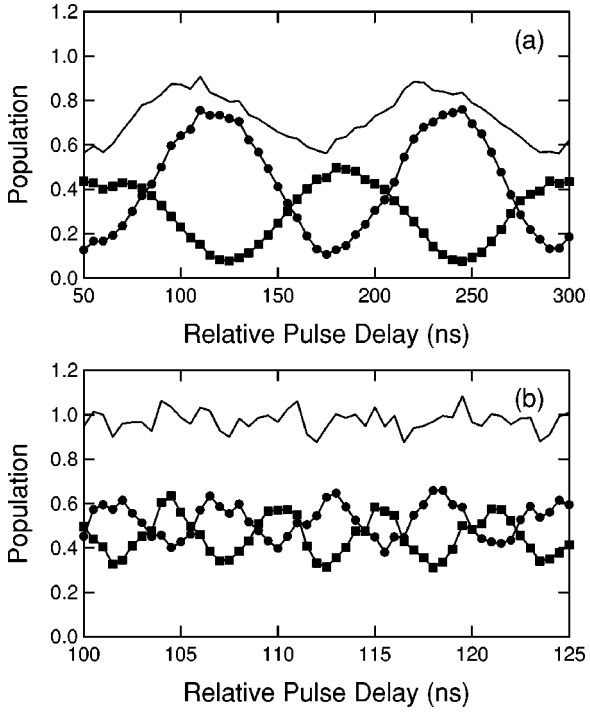

FIG. 3. Plot of population versus relative pulse delay between two half-cycle pulses in the (a) Na $23d_{3/2}$ (○) and $23d_{5/2}$ (□) states and (b) K $19d_{3/2}$ (○) and $19d_{5/2}$ (□) states. The line without symbols is the total field ionization signal.

tainty in the line center is 10–40 kHz at the 1σ level. The data for sodium, detailed in Table I, is in agreement with previous measurements, and has an error anywhere from a factor of 2 smaller than the best previous data [15] to a factor of 50 better than the best previous data [9,16]. Within the

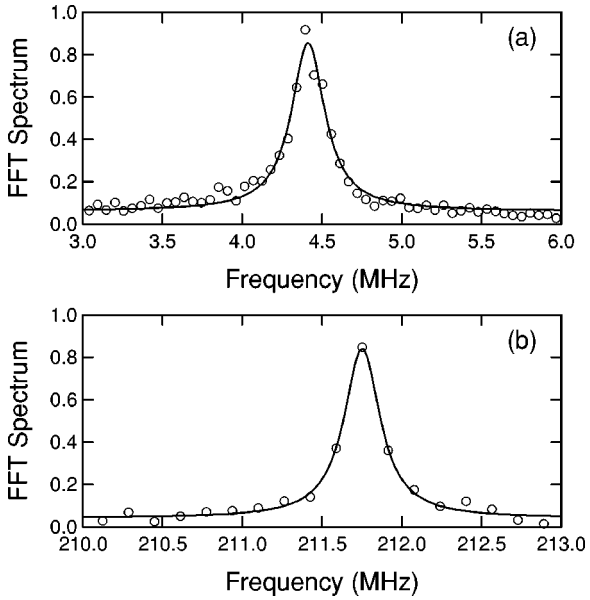

FIG. 4. Fourier transforms of time series like those shown in Fig. 3, for (a) Na $n=28$ and (b) K $n=18$. The solid line is a Lorentzian fit to the data which is used to determine the transition frequencies.

TABLE I. Fine-structure resonance frequences observed in this work. The quoted uncertainties are one standard deviation in the statistical uncertainty and the Stark uncertainties are the maximal shift assuming a static electric field of 70 mV/cm, determined from Eq. (4).

		σ(kHz)	
n	Δ_o(MHz)	Statistical	Stark
15	28.33	30	0.2
16	23.39	10	0.4
17	19.54	10	0.5
18	16.50	15	0.8
19	14.05	10	1.2
20	12.06	25	1.7
21	10.42	15	2.4
22	9.08	15	3.3
23	7.95	10	4.5
24	7.01	10	6.1
25	6.21	20	8.2
26	5.51	25	11
27	4.93	30	14
28	4.41	45	19
29	3.98	40	24
30	3.62	30	32
31	3.27	35	41
32	3.05	35	54
33	2.83	35	70
34	2.62	35	92

statistical uncertainty there is a small systematic offset of about 40 kHz between our data and that of Sun and MacAdam [15]. The source of the difference is not obvious but may be linked to their correction for residual Stark shifts. Because the fine structure is inverted stray fields would increase our measured frequencies, and there is no mechanism which we can think of which provides a systematic reduction in the observed frequency. The data for potassium, displayed in Table II, is also in agreement with previous measurements, but has an error more than ten times smaller and no systematic differences are observed [12,17].

It has been shown that fine-structure intervals in alkali atoms can be described by the empirical formula

$$\Delta_{\mathrm{fs}}=\frac{A}{(n-\delta)^3}+\frac{B}{(n-\delta)^5}+\frac{C}{(n-\delta)^7}, \tag{6}$$

where δ is the quantum defect of the state. In K, all three terms are used, while in Na, the first two suffice. We have used our measurements along with the previous best data in the range $n=4$ to 14 in Na [16,18] and $n=5$ to 36 in K [12,17] to determine the constants for these equations. The quantum defects used were those of the center of gravity of the doublet, calculated from the modified Rydberg–Ritz formula [1]. In Na, we determined that $A_{Na}=-97.57(2)$ GHz and $B_{Na}=+514.4(7)$ GHz. In K we found that $A_K=-1.1309(2)$ THz, $B_K=-15.57(5)$ THz, and $C_K=90.9(10)$ THz. Inclusion of our new data has reduced the errors in the A parameters by a factor of 2 from the most accurate previous result in Na [19] and a factor of 100 from the previous best result in K [17]. The B and C parameters have been improved by a smaller amount since they are mostly determined by the low lying levels.

TABLE II. Same as Table I but for potassium. The intervals for potassium were measured using the $m_j=3/2$ states, and the Stark uncertainties were calculated using Eq. (5).

		σ(kHz)	
n	Δ_o(MHz)	Statistical	Stark
17	253.30	40	0.1
18	211.75	10	0.1
19	178.87	20	0.2
20	152.48	20	0.3
21	131.04	30	0.4
22	113.50	40	0.6

IV. CONCLUSIONS

We have demonstrated a novel technique for using transitions driven by half-cycle pulses to make precise spectroscopic measurements in Rydberg atoms. The HCP-Ramsey method uses Stark shifts and state mixing, which are usually a source of uncertainty in multiphoton spectroscopy, to drive forbidden transitions and measure their field-free spacing. With this method we have determined fine-structure splitting frequencies ranging over two orders of magnitude. The precision of our measurements are limited mainly by the lifetime broadening of the states, and the spectral widths are comparable to other high resolution spectroscopic measurements of fine-structure in Rydberg atoms [15,20–23].

Transitions between fine-structure states are dipole-forbidden and hence direct transitions cannot usually be measured. In the past, the fine-structure intervals of Rydberg states have been measured by several other techniques: level crossing spectroscopy [18], fluorescence quantum beats [16,24], field-ionization quantum beats [25,26] radiofrequency resonance in a static field [9,12], and either optical or microwave resonance between the two fine-structure states and a common third state [15,20,22,17,27,28].

The major advantage of direct measurements is a relative insensitivity to stray electric fields: the major difficulty to be surmounted in precision measurements of Rydberg structure. Direct radiofrequency measurements of fine-structure intervals in zero static field requires multiphoton processes to drive the transitions, however, and in most multiphoton resonance experiments AC Stark shifts are significant and must either be calculated or data must be taken at several different power levels and the measured intervals extrapolated to zero power.

The HCP-Ramsey technique has proven to be a very effective method of directly measuring dipole forbidden transitions. Despite the use of fields that dramatically change the energy levels, the phase differences measured in the HCP-

Ramsey method depend only on the energy levels in the field free interval between the two pulses and these large Stark shifts are unimportant.

The experimental method is simple, efficient and accurate over a wide range of frequencies and can be used for many experiments on highly excited states of atoms and molecules. Because the transitions are driven by strong fields this method can be used to perform spectroscopy outside of the bandwidth of the HCP's and therefore could be extended to even larger and smaller frequencies. The largest frequency intervals that can be measured in the HCP-Ramsey method are limited only by the amplitude of the HCPs required to drive the transitions and stability of the pulse delay. The linewidth of the spectral features in these measurements is limited only by interaction time or finite state lifetime. Additionally, the strong fields can couple many states, and the energy differences between all pairs of states are present in the interferogram of any individual state, making this technique useful, for example, in situations where only one state can be selectively detected.

ACKNOWLEDGMENTS

We would like to thank Robert Jones and Duncan Tate for many useful discussions and Andreas Ostenwalder for a careful reading of the text. Peter Shapiro assisted with experiments to understand the potassium field ionization. M.C.D. was supported by Merck/Leighton.

[1] T.F. Gallagher, *Rydberg Atoms* (Cambridge University Press, Cambridge, 1994).
[2] E. Luc-Koenig, Phys. Rev. A **13**, 2114 (1976).
[3] R.M. Sternheimer, J.E. Rodgers, and T.P. Das, Phys. Rev. A **17**, 505 (1978).
[4] J.A.C. Gallas, G. Leuchs, H. Walther, and H. Figger, Adv. At., Mol., Opt. Phys. **20**, 413 (1985).
[5] R.R. Jones, C.S. Raman, D.W. Schumacher, and P.H. Bucksbaum, Phys. Rev. Lett. **71**, 2575 (1993).
[6] C.W.S. Conover and J. Rentz, Phys. Rev. A **55**, 3787 (1997).
[7] N. Rosen and C. Zener, Phys. Rev. **40**, 502 (1932).
[8] T.R. Dinterman and J.B. Delos, Phys. Rev. A **15**, 463 (1977).
[9] T.F. Gallagher, L.M. Humphrey, R.M. Hill, W.E. Cooke, and S.A. Edelstein, Phys. Rev. A **15**, 1937 (1977).
[10] T.F. Gallagher, L.M. Humphrey, W.E. Cooke, R.M. Hill, and S.A. Edelstein, Phys. Rev. A **16**, 1098 (1977).
[11] T.F. Gallagher and W.E. Cooke, Phys. Rev. A **19**, 694 (1979).
[12] T.F. Gallagher and W.E. Cooke, Phys. Rev. A **18**, 2510 (1978).
[13] N.L. Manakov and V.D. Ovsiannikov, J. Phys. B **10**, 569 (1977).
[14] V.A. Davydkin and V.D. Ovsiannikov, J. Phys. B **17**, L207 (1984).
[15] X. Sun and K.B. MacAdam, Phys. Rev. A **49**, 2453 (1994).
[16] C.M. Fabre, M. Gross, and S. Haroche, Opt. Commun. **13**, 393 (1975).
[17] D.C. Thompson, M.S. O'Sullivan, B.P. Stoicheff, and G-X. Xu, Can. J. Phys. **61**, 949 (1983).
[18] K. Fredriksson and S. Svanberg, J. Phys. B **9**, 1237 (1976).
[19] S. Dyubko, V. Efremov, S. Podnos, X. Sun, and K.B. MacAdam, J. Phys. B **30**, 2345 (1997).
[20] S. Dyubko, M. Efimrnko, V. Efremov, and S. Podnos, Phys. Rev. A **52**, 514 (1995).
[21] T.R. Gentile, B.J. Hughey, D. Kleppner, and T.W. Ducas, Phys. Rev. A **42**, 440 (1990).
[22] F. Merkt and H. Schmutz, J. Chem. Phys. **108**, 10 033 (1998).
[23] A. Osterwalder and F. Merkt, Phys. Rev. Lett. **82**, 1831 (1999).
[24] S. Haroche, M. Gross, and M.P. Silverman, Phys. Rev. Lett. **33**, 1063 (1974).
[25] G. Leuchs and H. Walther, Z. Phys. A **293**, 93 (1979).
[26] T.H. Jeys, K.A. Smith, F.B. Dunning, and R.F. Stebbings, Phys. Rev. A **23**, 3065 (1981).
[27] T.F. Gallagher, R.M. Hill, and S.A. Edelstein, Phys. Rev. A **13**, 1448 (1976).
[28] N.H. Tran, H.B. van Linden van den Heuvell, R. Kachru, and T.F. Gallagher, Phys. Rev. A **30**, 2097 (1984).